Wellbore Skin in Mine Dewatering and Drinking Water Supply: Field Observation, Mineralogy and Hydraulic Effect

Christoph Weidner[1], Georg Houben[1], Matthias Halisch[2], Stephan Kaufhold[1], Jürgen Sander[3], Morris Reich[4], Christian Menz[5]

[1]*Federal Institute for Geosciences and Natural Resources, BGR, Stilleweg 2, 30655 Hannover, Germany, Christoph.Weidner@bgr.de*
[2]*Leibniz Institute for Applied Geophysics, LIAG, Stilleweg 2, 30655 Hannover, Germany,*
[3]*Oldenburgisch-Ostfriesischer Wasserverband, OOWV, Georgstraße 4, 26919 Brake, Germany,*
[4]*RWE Power AG, Water Resources Management, Zum Gut Bohlendorf, 50126 Bergheim, Germany,*
[5]*Berlin Centre of Competence for Water, KWB gGmbH, Cicerostraße 24, 10709 Berlin, Germany*

Abstract

When it comes to well loss and efficiency, the occurrence of wellbore skin layers is one of the strongest influencing factors. Besides difficulties to remove the skin layer that is necessary during the drilling process, it is also not easily possible to determine if a skin layer is present in a well and whether or not it imposes a certain degree of well loss.

With this work, three types of skin layers are presented (surface cake, deep-bed filtration, layered cake in the aquifer), that have been observed at dewatering wells excavated in open-pits of the Rhenish lignite mining district in western Germany. Disturbed and undisturbed samples were analyzed for their geochemical and mineralogical composition in order to better understand the formation of the skin layer types and their fate during well operation.

Geochemical analysis revealed the skin layer to be mainly composed of quartz (≈ 40 wt-%), kaolinite/illite (≈ 30 wt-%), organic material (5-15 %) and secondary gypsum precipitates (up to 12.5 wt-%). Despite the high quartz contents, the granulometry yields high fractions of clay and silt (75-85 %). However, preferential flow paths, transecting the skin layer are created by micro-cracks and erosion-pathways which will cause a higher hydraulic conductivity than could be expected from the granulometry.

Key words: Wellbore Skin Layer, Well Loss, Drilling Mud Cake, Well Efficiency Optimisation, Mechanical Clogging, Particle Filtration, Formation Damage

Introduction

As several authors have concluded in recent literature, wellbore skin is a phenomenon that profoundly affects head losses of a well (Klauder 2010, Houben 2015a, b). Wellbore skin forms during water well drilling, when the drilling fluid infiltrates into the aquifer. Fine particles of the drilling mud (additives like bentonite or fines taken up from the penetrated layers) that cannot enter the pores of the aquifer are retained on the borehole wall. During the drilling process, especially in unconsolidated rocks, the formation of this thin but barely permeable layer is necessary to prevent major losses of drilling fluid into the aquifer and to ensure stability of the borehole. During the later well operation, however, the pressure loss resulting from a skin layer can easily reach values as high as the one of the surrounding aquifer itself (Houben 2015a, b).

It is thus all the more surprising, how little information can be found in the literature on the composition, hydraulic properties and mineralogy of such skin layers, based on actual field measurements or observations. Yeh and Chen (2007) even claim that direct measurements of skin thickness or other parameters are not possible at all. Most of the sparse experimental data available originates from drilling operations in the petroleum industry, which works under different p-T-conditions and generally applies several kinds of additives (Durand et al. 1996, Salehi et al. 2014) so these results are of limited comparability to water well applications.

This study now focuses on descriptions and (undisturbed) sampling of skin layers, observed in water wells for open-pit dewatering as well as drinking water supply, where different types of skin layers should be expected. As wells for drinking water supply are generally constructed to last as long as

possible – with service lives of up to 50 years – huge efforts are invested in a proper (hydromechanical) well development, in order to remove the drilling mud cake after well installation. In contrast, for mine dewatering in the Rhenish lignite district in Germany, a huge number of wells are needed to enable dry surface mining and to ensure slope stability of the open-pits. As the open-pit progresses, following the directions of the resource, dewatering wells in the pre-field eventually are excavated after design service-lives of 5 to 10 years or less. Thus, not much effort is put into well development, as the wells are generally operated at maximum capacity from the beginning anyway. Lately, for mine dewatering applications, the concept of intermittent abstraction (van Beek et al. 2010) has been found to be a successful alternative to conventional well development (Reich & Menz 2015). But also no chemical or particular additives (but only water) are used in the drilling fluid. Still, the tremendous hydraulic effect of the skin layer legitimates considerations about its formation and composition. Especially, when a large number of wells are needed to facilitate secure mining of natural resources or sustainable supply of high quality drinking water, there is a huge potential for cost reduction and energy savings through optimisation of well yield and efficiency.

Thus, within this work we present a direct observation, microscopic investigation and geochemical-mineralogic analyses of wellbore skin samples at five excavated open-pit dewatering wells in the Rhenish lignite district in W Germany and at one drinking water supply well in NW Germany, accessed by inclined core drilling (Tab. 1).

Table 1 *Wells included in the investigation (ststw: stainless steel wire screen, ppfg: prepacked fiber glass rod screen; ac: asbestos cement; Cu: copper; [*]): sample taken in cased section; hz.: regional geologic horizon; hz. 6B/D: shallow marine anoxic loose fine to medium sand; hz. 7: shallow marine anoxic loose medium sand; hz. 8: terrestrial, fluvial oxic terrace loose fine to medium gravel; quaternary: terrestrial medium to fine sand, light grey; P: Photo; M: electron and polarizing microscope; X: XRD and XRF; CT: computer tomography).*

Well	Location	Service life [yrs]	Sample [m bgl]	Screen [m bgl]	Screen type	Lithology	Analytics
WS5015	Garzweiler	< 10	≈ 100	93-108	ststw	hz. 6D	P, M, X, CT
WS5315	Garzweiler	< 5	≈ 100	102-108	ppfgr[*]	hz. 6D	P, X
WS3151	Garzweiler	< 10	140	133,5-142,5	ststw	hz. 6B	P
HS41	Hambach	> 20	230	229-242	ac	hz. 7	P, CT
HS1059	Hambach	< 10	267	297-309	ppfgr[*]	hz. 7/8	P
Well 31	Großenkneten	> 40	34.5	29-59	Cu	quaternary	P

Methods

At all six wells, photo documentations were conducted to compare the macroscopic characteristics of different skin-layer types. At three wells, disturbed and undisturbed samples were taken to allow for microscopic and/or mineralogical analysis by cored drilling (Fig. 1, center), core cutter rings (Fig. 1, left), and epoxy resin impregnation (Fig. 2).

For sample stabilization and preparation of thin sections and test pieces for SEM and CT analyses, the samples were impregnated with the epoxy compound Araldite® 2020 (XW 396/XW 397; density = 1,1 kg/m^3, viscosity = 150 mPa). Transmitted light microscopy analysis was applied to evaluate petrography on covered thin sections with a Zeiss Axioplan polarising microscope, supported by Zeiss Axiovision Software. An Environmental Electron Scanning Microscope (ESEM) of the type FEI Sirion D1625 (low vacuum, 0.6 mbar) was used to investigate samples of the borehole wall. Porosity determination and 3D-imaging was accomplished with a nanotom S 180µ-CT (GE Sensing & Inspection Technologies GmbH,Wunstorf, Germany) (tube characteristics: 180 kV, 500 mA). The 3D image data were processed with the AVIZO Fire software suite (Visualization Sciences Group). Measurements of hydraulic conductivity were taken from experimental data core cutter ring samples by Houben (2015a, b).

X-ray diffraction (XRD) was conducted with a PANalytical X'Pert PRO MPD Θ-Θ diffractometer (Cu-Kα) with variable divergence slit, soller collimators, and Scientific X´Celerator position sensitive detector (active length 0.59°). Samples of 28 mm diameter were investigated from 2° to 85° 2Θ (step

size: 0.0167°; counting time: 10 s). Overnight treatment with ethylene glycol vapor was applied to investigate swelling clay minerals qualitatively by comparative XRD patterns (oriented aggregate mound, fraction < 2 µm).

Figure 1 *Inclined drilling into the annulus of a decommissioned water supply well in Großenkneten (centre) and undisturbed sampling at excavated open-pit dewatering wells in the lignite open-pits Garzweiler and Hambach (left and right).*

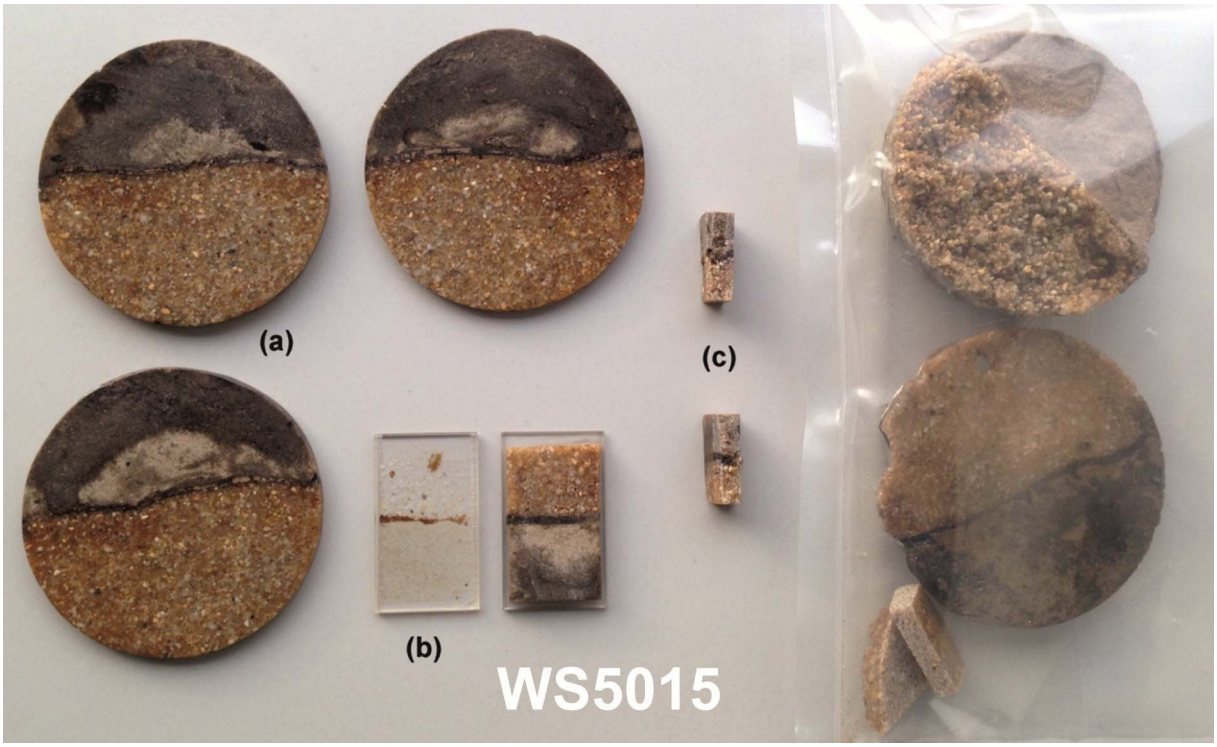

Figure 2 *Prepared specimens of an undisturbed sample from Well WS5015: core cutter ring sample, impregnated with epoxy and cut into slices (a) for thin section preparation (b), ESEM and CT inspection (c).*

Loss on ignition (LOI) was determined by heating 1 g of sample material to 1030°C for 10 min and subsequent weighing. Powdered samples were mixed with lithium metaborate (Spectroflux, Alfa Aesar) as flux material for subsequent glass conversion within 20 min at 1200°C. Wavelength dispersive X-Ray Fluorescence spectrometry (WD-XRF) was then applied to determine chemical composition with a PANalytical Axios and a PW2400 spectrometer.

For total carbon and sulphur contents, 170-180 mg of air-dried sample material were grinded and heated to 1800-2000°C in an oxygen atmosphere in order to expel carbon and sulphur as CO_2 and SO_2 gas which was then detected with an infrared detector of a LECO CS-444-Analyser. The procedure was repeated with a sample, pre-treated with hydrochloric acid at 80 °C until inorganic carbon contents were expelled (no further gas evolution) in order to determine the organic carbon content (C_{org}). Inorganic carbon (C_{inorg}) was then derived as the difference between total and organic carbon.

Results

Within the six samples, three different types of skin layers could be distinguished. A wellbore surface cake could be observed in three cases (Fig. 3.A), deep bed filtration occurred in one case (Fig. 3.B) and in another case the fines had invaded the aquifer material to be deposited at about 1 cm from the borehole wall (Fig. 3.C). In the case of the drinking water supply well, no skin layer was observed (Fig. 3.D).

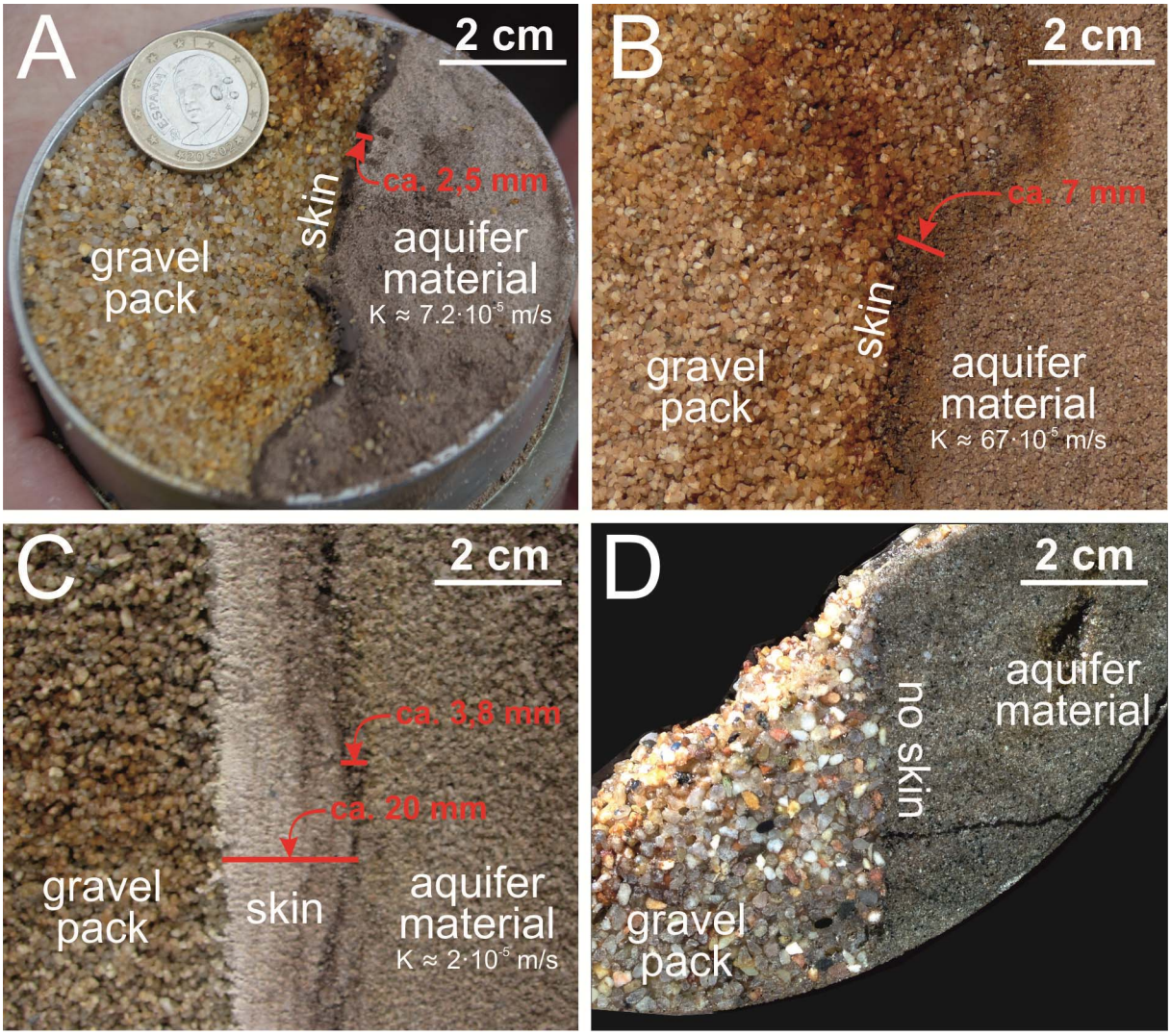

Figure 3 *Types of skin layers observed. A: wellbore surface cake (well WS5015, open-pit Garzweiler, RWE Power AG), B: deep-bed filtration (well HS41, open-pit Hambach, RWE Power AG), C: outer filter cake (well HS1059, open-pit Hambach, RWE Power AG), D: no skin (well 31, Großenkneten, OOWV).*

Polarizing microscopy of the thin section of sample WS5015 (Fig. 4) revealed the skin layer to be a densely packed brownish surface cake layer of up to 2 mm in thickness in between the finely sandy aquifer and the fine gravel pack materials. Within the skin layer, no singular mineral grains, but several micro-cracks could be identified. Detailed ESEM imagery of the skin layer (Fig. 5) showed an intricate assemblage of angular grains (mostly quartz) and platy clay and silt minerals. Electron microscopy, XRD and XRF revealed the skin layer of the surface cake samples WS5015 and WS5315 to be mainly composed of quartz with accessory components of kaolinite and muscovite/illite withtraces of feldspars, carbonate, chlorite, and organic matter as well as secondarily formed gypsum. No significant contents of expansive clays, e.g. smectite could be identified (Tab. 2-4).

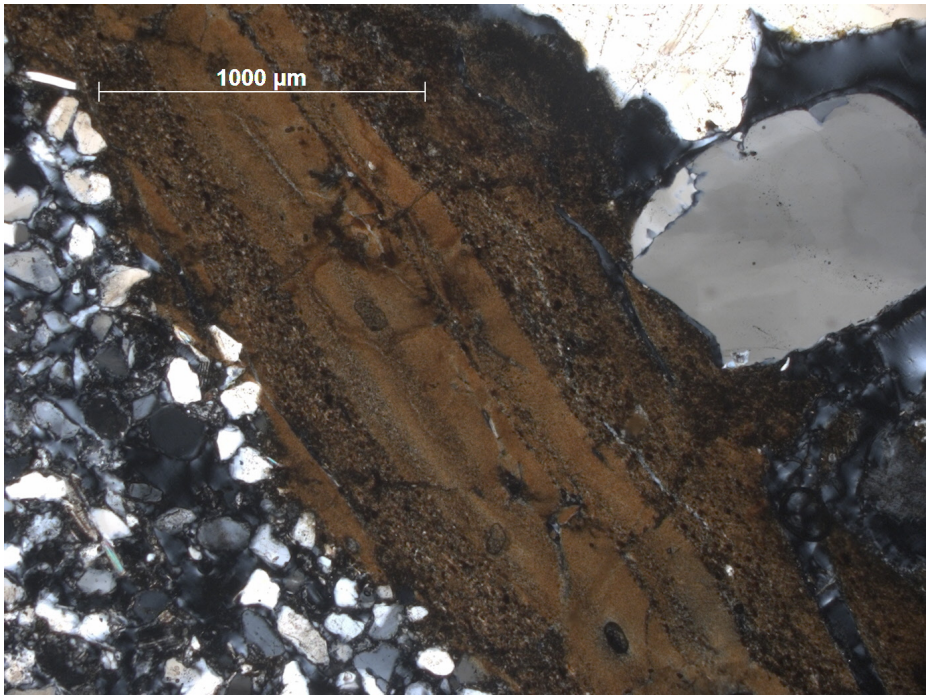

Figure 4 *Detail image of thin section of the former borehole wall of well Garzweiler WS5015 (screened well section; polarized light). The coarse rounded grains in the upper right corner represent the gravel pack, the smaller, more angular grains to the left represent the fine sand aquifer. The skin layer is visible in between as a brown laminated layer with varying grain sizes and microscopic cracks in different directions.*

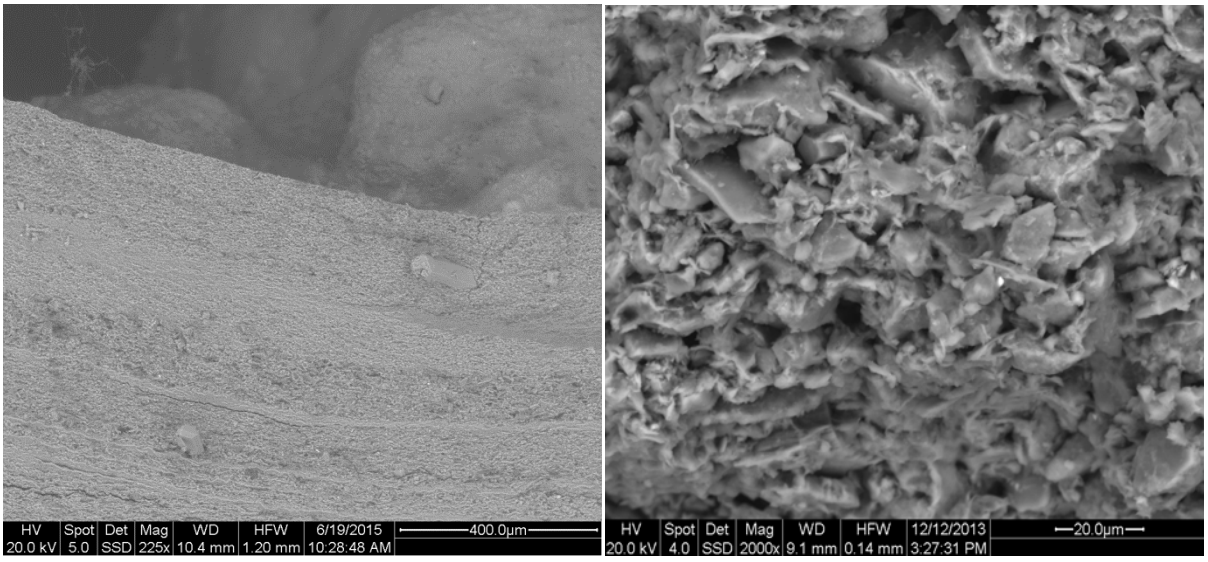

Figure 5 *Fine grained matrix with coarse secondary gypsum crystals in an overview ESEM image of the wellbore surface cake from well WS5315 (left) and detailed ESEM image of the fine-grained skin layer matrix (mostly quartz) of the wellbore surface cake from well WS5015 (right).*

Contrary to the WS5015 specimen, no distinct skin layer can be identified in the 2D CT cross section of sample HS41 (Fig. 6). Instead, fine particles have migrated into the aquifer material (Fig. 6, top) and form a deep-bed filtration layer. Within this layer, open and connected pores can be found (dark grey to black areas), showing that both aquifer and gravel pack, are hydraulically connected. Nevertheless, the hydraulic conductivity of the particle-invaded aquifer presumably is significantly lower than the conductivity of the undisturbed aquifer material. Digital image analysis (pore distribution and visualization) could not be performed, due to the overlapping grey values (i.e. similar absorption coefficients of the materials) of the resin and of the fine particles present in the pore spaces of the aquifer which had been possible for the WS5015 sample (Houben et al. 2016). The CT images of HS41 do not give information on when and from where the particles invaded. They could have accumulated during the drilling process (invasion of particles suspended in drilling fluid), as their color indicates but also through a later migration of aquifer fines towards the well during operation ("secondary filtration" or "mechanical wellbore clogging", cf. van Beek et al. 2010 and Reich & Menz 2015).

Table 2 *Mineralogy of skin samples, determined by qualitative XRD analysis*

Sample	Main components	Accessory components
WS5015	quartz	muscovite-illite, kaolinite, sodium feldspar, smectite/mixed layer
WS5315	quartz	gypsum, muscovite-illite, kaolinite/chlorite, potassium feldspar
HS41	quartz	microcline, orthoclase

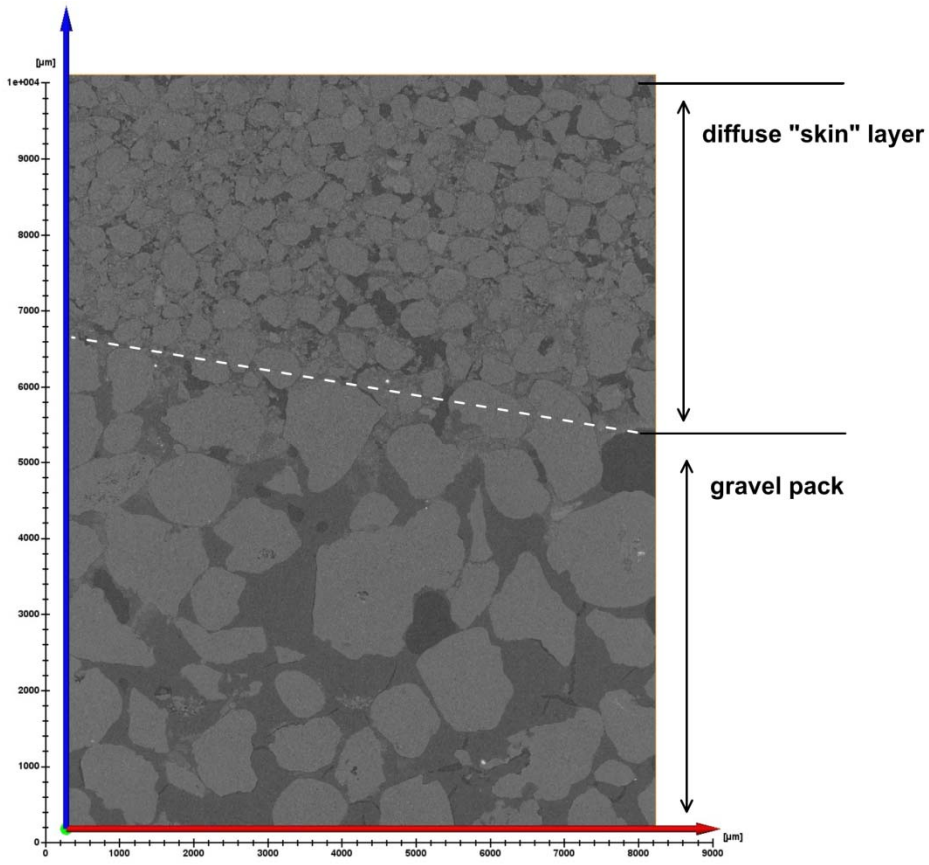

Figure 6 *2D CT cross section of sample HS41 (z-y plane: 9.94 x 7.85 mm). Contrary to sample WS5015, no distinct skin layer can be found. Instead, an invasion of fine particles into the pore space of the aquifer is visible in the upper part.*

From the XRF results, the mineralogical composition can be estimated from a simplified nominal mineralogy of only quartz and kaolinite. Stoichiometrically incorporating all aluminum into kaolinite ($Al_2[(OH)_4Si_2O_5]$), the remaining silicon is consumed for quartz (SiO_2). Other elements form

iron/manganese oxides, sulfates/sulfides, carbonates and organics. Nominal compositions yield 7.72 mol/kg quartz (or 46.4 wt.-%) and 1.36 mol/kg kaolinite (or 35.1 wt.-%) in sample WS5015 and 6.85 mol/kg quartz (or 41.2 wt.-%) and 1.13 mol/kg kaolinite (or 29.1 wt.-%) in sample WS5315. The concentrations of inorganic carbon indicate a minor importance of carbonates in both samples (Tab. 3). A noticeable content of sulphur is present in WS5315 which, according to XRD and electron microscopy, appears as gypsum (12.6 wt.-% of $CaSO_4 \cdot 2H_2O$). Assuming a nominal composition of CH_2O, organic carbon corresponds to 4.65 and 14.5 wt.-%, in the samples WS5015 and WS5315, respectively, and is probably responsible for the brown color. The higher loss on ignition for sample WS5315 indicates higher contents of thermally instable phases such as gypsum and organic matter.

Table 3 *Geochemistry of skin samples WS501 and WS5315 as well as aquifer material samples HS41_u (unaltered aquifer material) and HS41+p (aquifer material invaded by fine particles) (LOI: loss on ignition)*

[wt.-%]	SiO_2	TiO_2	Al_2O_3	Fe_2O_3	MnO	MgO	CaO	Na_2O	K_2O	C_{inorg}	C_{org}	S	LOI
WS5015	62.7	0.78	13.9	6.22	0.017	1.06	0.84	0.39	2.34	0.04	1.86	0.19	11.3
WS5315	54.7	0.62	11.5	5.67	0.029	0.76	0.85	0.22	1.83	0.09	5.79	2.35	23.0
HS41_u	95.9	0.04	2.1	0.10	0.001	0.03	0.05	0.14	1.05	0.01	0.06	0.02	0.50
HS41+p	95.2	0.07	2.3	0.24	0.001	0.02	0.08	0.15	1.11	0.01	0.14	0.03	0.79

For the deep-bed filtration case of well HS41, the chemical composition of the unaltered aquifer and the aquifer affected by particle invasion were compared (Tab. 4). The XRD analysis of both samples indicated quartz as main phase, with traces of potassium feldspar. Only slight increases in LOI and C_{org} adumbrate a barely measurable invasion of organic particles. But the majority of invading particles therefore must be chiefly quartz as well.

In comparison to these mineralogical results, granulometric analyses and permeameter tests by Houben et al. (2016) resulted in high contents of clay and silt of about 75 % in the skin layer and a low measured hydraulic conductivity of $6.2 \cdot 10^{-6}$ m/s (WS5015). Still, this conductivity is significantly higher than should be expected from a poorly sorted silt and clay-rich sample, which is probably due to conductive micro-cracks transecting the skin layer and therefore creating preferential flow paths through the layer.

Conclusions

In conclusion, the typology of skin layers was found to vary significantly, even in a small number of samples. Even though very fine granulometries were measured by Houben et al. (2016), with > 40 wt-% quartz is the main component of the skin layer, accompanied by around 30 % of kaolinite/illite. Despite the overall lignitic environment, organic carbon contents appear to play only a minor role (5 to 15 %). Secondary gypsum precipitation can occur in the environment of pyrite oxidation and later neutralization by calcite.

With evaluation of the CT results, calculations of the pressure field and concentration of flow lines throughout the pore space are planned for the near future followed by calculation of the filtration process and buildup of the mud cake itself. Even an experimental reconstruction of mudcake buildup and its removal by (intermittent) backflow (normal abstraction, well development) is thinkable. Such investigations could help to understand the field observations by RWE Power AG of well efficiencies increasing by more than 10 % as a result of intermittent abstraction (Reich & Menz 2015).

Even very thin skin layers were found to cause a significant reduction of hydraulic conductivity of the whole system, though distinct structural properties like micro-cracks or skin erosion can possibly help to maintain a high well yield. Altogether, significant improvements should be expected from further studies on the effectivity of measures to remove the drilling mud cake (like well development) or to prevent its formation in the first place.

Acknowledgements

Thanks go to the Oldenburgisch-Ostfriesischer Wasserverband (OOWV) and RWE Power AG for the opportunity to take borehole wall samples from the aquifer/gravelpack-interface by well overcoring and access to the open-pits. Constructive suggestions of the reviewers were very much appreciated.

References

van Beek K, Breedveld R, Tas M, Kollen R (2010) Prevention of Wellbore Clogging by Intermittent Abstraction. Ground Water Monitoring & Remediation 30(4):81—89

Durand C, Lecourtier J, Rosenberg E, Loeber L (1996) Relationship between composition, structure and permeability of drilling filter cakes. Revue de l'Institut Francais du Petrole 51(6):777—788

Houben GJ (2015a) Review: Hydraulics of water wells—flow laws and influence of geometry. Hydrogeology J 23(8):1633—1657

Houben GJ (2015b) Review: Hydraulics of water wells—head losses of individual components. Hydrogeology J 23(8):1659—1675

Houben GJ, Halisch M, Kaufhold S, Weidner C, Sander J, Reich M (2016): Analysis of Wellbore Skin Samples – Typology, Composition, and Hydraulic Properties. Groundwater, online first – [doi: 10.1111/gwat.12403.]

Klauder W (2010) Experimentelle Untersuchung der Anströmung von Vertikalfilterbrunnen. PhD, Civil Engineering, RWTH Aachen University, 240 pp.

Reich M, Menz C (2015) Overview of technical developments in opencast mine drainage at RWE Power AG. World of mining 67(6):398—408

Salehi A, Hussmann S, Karimi M, Ezeakacha C, Tavanei A (2014) Profiling drilling fluid's invasion using scanning electron microscopy: implications for bridging and wellbore strengthening effects. Society of Petroleum Engineers SPE-170315-MS.

Yeh H-D, Chen Y-J (2007) Determination of skin and aquifer parameters for a slug test with wellbore-skin effect. J Hydrol 324(3-4): 283—294